Identification of inorganic and organic species of phosphorus and its bio-availability in nitrifying aerobic granular sludge

Wenli Huang[a], Wei Cai[a], He Huang[a], Zhongfang Lei[a,*], Zhenya Zhang[a,*], Joo Hwa Tay[b], Duu-Jong Lee[c]

[a] Graduate School of Life and Environmental Sciences, University of Tsukuba, 1-1-1 Tennodai, Tsukuba, Ibaraki 305-8572, Japan

[b] Department of Civil Engineering, Schulich School of Engineering, University of Calgary, 2500 University Drive NW, Calgary, Canada

[c] Department of Chemical Engineering, National Taiwan University, Taipei 106, Taiwan

GRAPHICAL ABSTRACT

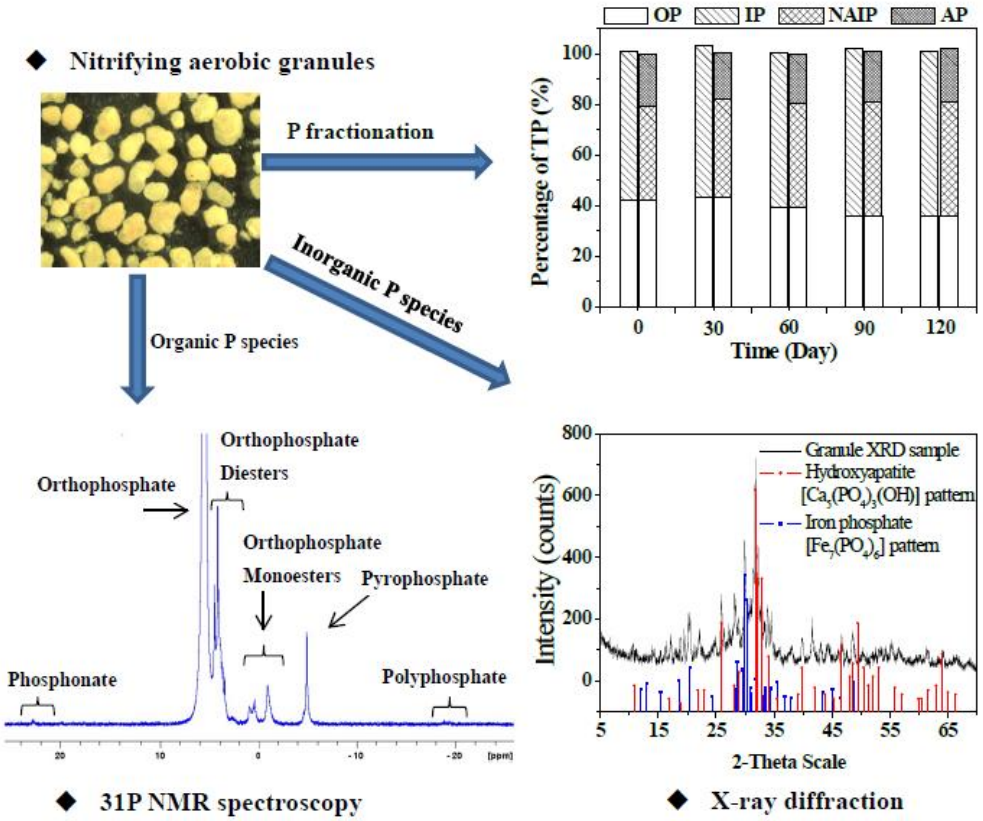

* Corresponding author.
Tel/fax.: +81 29 853 6703. E-mail address: lei.zhongfang.gu@u.tsukuba.ac.jp (Z. Lei)
Tel./fax: +81 29 853 4712. E-mail address: zhang.zhenya.fu@u.tsukuba.ac.jp (Z. Zhang)

Abstract

Phosphorus (P) recovery from sewage sludge is necessary for a sustainable development of the environment and thus the society due to gradual depletion of non-renewable P resources. Aerobic granular sludge is a promising biotechnology for wastewater treatment, which could achieve P-rich granules during simultaneous nitrification and denitrification processes. This study aims to disclose the changes in inorganic and organic P species and their correlation with P mobility and bio-availability in aerobic granules. Two identical square reactors were used to cultivate aerobic granules, which were operated for 120 days with influent ammonia nitrogen (NH_4-N) of 100 mg/L before day 60 and then increased to 200 mg/L during the subsequent 60 days (chemical oxygen demand (COD) was kept constant at 600 mg/L). The aerobic granules exhibited excellent COD removal and nitrification efficiency. Results showed that inorganic P (IP) was about 61.4 - 67.7% of total P (TP) and non-apatite inorganic P (NAIP) occupied 61.9 - 70.2% of IP in the granules. The enrichment amount of NAIP and apatite P (AP) in the granules had strongly positive relationship with the contents of metal ions, i.e. Fe and Ca, respectively accumulated in the granules. X-ray diffraction (XRD) analysis and solution index calculation demonstrated that hydroxyapatite ($Ca_5(PO_4)_3(OH)$) and iron phosphate ($Fe_7(PO_4)_6$) were the major P minerals in the granules. Organic P (OP) content maintained around 7.5 mg per gram of biomass in the aerobic granules during the 120 days' operation. Monoester phosphate (21.8 % of TP in extract), diester phosphate (1.8%) and pyrophosphate (0.1%) were identified as OP species by Phosphorus-31 nuclear

magnetic resonance (^{31}P NMR). The proportion of NAIP+OP to TP was about 80% in the granules, implying high potentially mobile and bio-available P was stored in the nitrifying aerobic granules. The present results provide a new insight into the characteristics of P species in aerobic granules, which could be helpful for developing P removal and recovery techniques through biological wastewater treatment.

Keywords:
Aerobic granules; Nitrification; P fractionation; Phosphorus-31 nuclear magnetic resonance (^{31}P NMR)

1. Introduction

Phosphorous (P) is an essential and limiting element for living organisms and human beings, especially for the growth of plants. P deficiency will greatly affect and restrict crop yields worldwide. However, phosphate rock, a non-renewable resource and raw material used for P fertilizers, is reported to be depleted in 50-100 years (Cordell et al., 2009). Thus P resource protection and P recovery is prerequisite for a sustainable agriculture and society on a global scale. On the other hand, sewage sludge generated from wastewater treatment is regarded as a potential phosphorus reservoir due to its high production amount and high P content (Xu et al., 2012). Land application of sewage sludge as P fertilizer has become one of the main sludge disposal practices (Singh and Agrawal, 2008; Xie et al., 2011a).

Aerobic granular sludge is a promising biotechnology for nitrogen and

phosphorus removal from wastewater. The aerobic granules possess advantages like excellent settleability, high biomass and ability to withstand high loading rate compared to conventional activated sludge processes (Qin et al., 2004; Yilmaz et al., 2008; Adav et al., 2008a). Previous studies indicate that P-rich aerobic granules could be achieved during simultaneous nitrification and denitrification processes (Lin et al., 2012; Li et al., 2014), implying that aerobic granular sludge can be more prospectively used for P fertilizer after being properly treated.

As well known that not all the forms of P exhibit similar mobility and bio-availability in the sludge, detailed information about P fraction is necessary for both activated sludge and aerobic granules, especially when land application of sludge is taken into consideration. Moreover, identification of P species in aerobic granular sludge is helpful to understand the characteristics and function of P in aerobic granules and thus the mechanisms of P removal through this new biotechnology. For this purpose, some researchers declared that sewage sludge contained higher mobilizable forms of P, i.e. non-apatite inorganic P than sediment (Medeiros et al., 2005; Xie et al., 2011a and 2011b), which is much meaningful for land application of sewage sludge. To date, as for aerobic granules, lab-scale experiments have been conducted on the mineral forms of P, demonstrating that the major inorganic P species in aerobic granules were greatly dependent on influent characteristics and operation conditions (Angela et al., 2011; Lin et al., 2012; Li et al., 2014). More specifically, in enhanced biological phosphorus removal (EBPR) process, biologically induced precipitation of phosphorus as hydroxyapatite was discovered in the core of granules

(Angela et al., 2011). On the other hand, Ca-Mg phosphate and whitlockite ($Ca_3(PO_4)_2$) were found to be the major minerals in aerobic granular sludge used for simultaneous phosphorus accumulation by chemical precipitation and biological nitrogen removal via nitrite (Li et al., 2014). In addition, previous works show that orthophophosphate, pyrophosphate and polyphosphate are the main inorganic species of phosphorus in the EPS of activated sludge and aerobic granular sludge, accounting for 5-10.5% of total P in the EBPR systems (Zhang et al., 2013a, 2013b). However, the organic P species in aerobic granules, the potential available P resource closely related with the activity of phosphate accumulating organisms (PAOs) (Uhlman et al., 1990), is poorly understood most probably attributable to its complex nature and the limitation of analytical methods.

Recent research indicates that phosphorus-31 nuclear magnetic resonance spectroscopy (^{31}P NMR) can be used for analyzing inorganic and organic P species (orthophosphate monoesters, orthophosphate diester and phosphonates) in sediments, soil and activated sludge since it is able to distinguish multiple P compounds among complex substances (Uhlmann et al., 1990; Ahlgren et al., 2011; Li et al., 2013). Therefore it is speculated that this technology could provide more insight into the P species in aerobic granules, especially the organic P fraction.

This study aims to reveal the fractionation and distribution of P in aerobic granules and to evaluate the mobility and bio-availability of P in aerobic granules. In addition, organic and inorganic P species in the granules were also determined and characterized by ^{31}P NMR and X-ray diffraction (XRD), respectively. It is expected

that this work would not only be useful for P utilization and recovery from aerobic granules but also provide insight into the characteristics of P in aerobic granules, which will help to develop applicable technologies for P removal and recovery from wastewater.

2. Materials and methods

2.1. Experimental set-up and operation

Aerobic granules were cultivated in two identical sequencing batch reactors (SBRs) made of acrylic plastic with height of 60 cm and square cross section of 6 cm×6 cm. Their effective working volume was 1.4 L. Aeration was provided by an air pump (AK-30, KOSHIN, Japan) through air bubble diffusers at the bottom of each reactor with an air flow rate of 2.0 cm/s and the dissolved oxygen (DO) maintained at 7-9 mg/L during aeration. Synthetic wastewater was used in this study, and its composition was as follows: chemical oxygen demand (COD) 600 mg/L (50% of which was contributed by glucose and sodium acetate, respectively); 10 mg PO_4-P/L (KH_2PO_4); 100 mg NH_4-N/L (NH_4Cl) during the first 60 days' operation and then increased to 200 mg NH_4-N/L till the end of experiment; 10 mg Ca^{2+}/L ($CaCl_2$); 5 mg Mg^{2+}/L ($MgSO_4 \cdot 7H_2O$); 5 mg Fe^{2+}/L ($FeSO_4 \cdot 7H_2O$); and 1ml/L of trace element solution. The trace element solution contained (in mg/L) H_3BO_3 (50), $ZnCl_2$ (50), $CuCl_2$ (30), $MnSO_4 \cdot H_2O$ (50), $(NH_4)_6Mo_7O_{24} \cdot 4H_2O$ (50), $AlCl_3$ (50), $CoCl_2 \cdot 6H_2O$ (50), and $NiCl_2$ (50) (Adav et al., 2008b). The pH in the reactors was adjusted with sodium bicarbonate to be within 7.5-8.0.

123 Each reactor was inoculated with 0.5 L of seed sludge sampled from a
124 sedimentation tank of the Shimodate Sewage Treatment Plant, Ibaraki Prefecture,
125 Japan. The initial mixed liquor suspended solids (MLSS) concentration was 4.6 g/L
126 with sludge volume index (SVI) of 81.4 ml/g and MLVSS/MLSS of 0.8 in the two
127 reactors. After aerobic granules appeared, the mixed liquor was withdrawn daily from
128 the reactors in order to keep their solids retention time (SRT) around 40 days. The
129 reactors were operated sequentially in a 4-h cycle at room temperature (25±2℃): 2
130 min of influent filling, 28 min of non-aeration period, 186-206 min of aeration, 2-20
131 min of settling, and 4 min of effluent discharge. The settling time was gradually
132 decreased from 20 min to 2 min due to the increase in settleability of the sludge. The
133 volumetric exchange ratio was kept at 54%, resulting in a hydraulic retention time of
134 7.4 h.

135 **2.2. Chemical and physical analysis**

136 Mixed liquor (volatile) suspended solids (ML(V)SS), sludge volume index (SVI),
137 COD, ammonia nitrogen (NH_4-N), nitrite nitrogen (NO_2-N), nitrate nitrogen (NO_3-N),
138 and phosphorus (PO_4-P) were measured in accordance with standard methods
139 (APHA,1998). DO concentration in the bulk liquid was measured with a DO meter
140 (HQ40d, HACH, USA). pH was determined by using a pH meter (Mettler Toledo
141 FE20, Switzerland).

142 Metal ions in sludge particles were quantified after the sludge samples being
143 digested and filtered through 0.22 μm cellulose nitrate membrane filters (Nalgene).
144 0.1 g of dried sludge was digested in a mixture of 3 ml hydrochloric acid (37%,

145 Wako), 1 ml nitric acid (70%, Wako), and 1 ml perchloric acid (60%, Wako) on an
146 electric heating plate for 10 min. The concentration of each metal was measured by
147 inductively coupled plasma mass spectrometry (ICP-MS, ELAN DRC-e, Perkin
148 Elmer, USA). Granular surface elemental analysis was also performed by using an
149 energy dispersive X-ray - spectroscopy (EDX) equipped with a JSM 7000F field
150 emission scanning electron microscope (FE-SEM) operated at an acceleration voltage
151 of 20 kV.

152 The mean granular size was measured by a stereo microscope (STZ-40TBa,
153 SHIMADZU, Japan) with a program Motic Images Plus 2.3S (Version 2.3.0).
154 Morphology characteristics of the granules were observed using a scanning electron
155 microscope (SEM, JSM6330F, Japan). XRD analysis was performed using a
156 Multiflex diffractometer (Rigaku, Japan) with a cobalt tube scattering from 5 to 75° in
157 2θ. The samples used for XRD analysis were previously dried and calcined in an oven
158 at 500℃ for 2 h in order to remove the organic fraction.

159 Average values were taken for all the determinations and used for results and
160 discussion.

161 **2.3. Phosphorus fractionation in granular sludge**

162 In this study, the Standards, Measurements and Testing (SMT) Programme extraction
163 protocol was applied to analyze phosphorus fractions in the aerobic granules, which
164 has been widely used in soil, sediment and sewage sludge samples (Ruban et al., 1999;
165 Medeiros et al., 2005). After sequential extraction based on the SMT method,
166 phosphorus in sludge can be fractionated into the following 5 categories: (1)

concentrated HCl-extractable P, namely total P (TP), (2) organic P (OP), (3) inorganic P (IP), (4) non-apatite inorganic P (NAIP, the P fraction associated with oxides and hydroxides of Al, Fe and Mn), and (5) apatite P (AP, the P fraction associated with Ca). In order to avoid the transformation of P species in granules during preparation, the samples taken from the reactors were frozen immediately at -80℃, lyophilized and stored at -20℃ until analysis. The phosphorus concentration in the supernatant collected after extraction was determined with molybdenum blue method.

2.4. ^{31}P NMR analysis

Granular sludge taken from each reactor was also frozen immediately at -80℃, lyophilized, and ground to fine powders. Then P was extracted from 2 g of the prepared sludge powder with 40 ml of a solution consisting of 0.25 M NaOH and 0.05 M Na_2EDTA(Turner et al., 2003). The mixture was shaken for 6 h at 100 rpm and ambient temperature and then centrifuged at 6000×g for 20 min at 4℃. 2 ml of the resultant supernatant was taken for TP, IP and OP analysis. The remaining extracts were freeze-dried again and stored at -20℃ till ^{31}P NMR analysis.

500 mg of freeze-dried extract was re-dissolved in 0.8 ml of 1M NaOH and 0.2 ml D_2O and then transferred to a 5 mm NMR tube. The ^{31}P NMR spectrum was obtained by using a Bruker Avance-600MHz NMR Spectrometer at 242.94 MHz for ^{31}P. 90℃ of pulse width, 25℃ of regulated temperature, and acquisition time of 0.67 s (with relaxation delay of 2s) were applied in the experiments. Chemical shifts of signals were determined relatively to an external standard of 85% H_3PO_4 via signal lock. The peaks were assigned to P species according to the reports in literature with

peak areas calculated by integration (Ahlgren et al., 2005; Turner et al., 2003; Turner, 2004; Zhang et al., 2013).

3. Results and discussion

3.1. Formation and characterization of aerobic granules

The SBRs were operated for 120 days. Granules appeared in the two reactors on day 13 after startup and then grew gradually along with the operation. From day 90 on, the granular size averagely stabilized at 0.76-0.78 mm, although the initial diameter of seed sludge was about 0.17 mm (Table 1). This observation is in agreement with the finding by Verawaty et al. (2013) who reported that granules in the reactor equilibrated towards a common critical size of around 0.6-0.8 mm. MLSS and SVI_{30} were determined to be 12-13 g/L and 22 ml/g after 60 days' cultivation. It is worth noting that the MLVSS/MLSS ratio of granules progressively decreased from 86% to 73% at the end of experiment, probably due to the accumulation of mineral substances, which will be further demonstrated in the following sections. As shown in Fig. 1a, the yellowish mature granules had irregular shapes, possibly contributed by the square structure of SBRs in this study. SEM observation on day 110 clearly shows the compact and dense structure of the granules, and most of the bacteria are distributed in the outer layer (Figs. 1b and 1d) with little bacteria in the core of the granules (Figs. 1b and 1c), which is in agreement with the results from Adav et al. (2008b). Furthermore, EDX results shown in Fig. S1 indicate that the intensities of metal ions and P are decreasing along with the granular radius, signaling the metal ions and P are

mainly accumulated in the core of granules. This observation suggests the existence of some relationship between the accumulated metal ions and phosphorus.

3.2. Overall pollutants removal performance

In order to evaluate COD, ammonia and phosphate removal rates, typical batch experiments were carried out on days 55 and 115, namely the influent NH_4-N concentration was 100 mg/L and 200 mg/L, respectively (Fig. 2). It was found that COD removal efficiency was about 80% during non-aeration stage, then increased to around 92% after aeration for 30 min and kept this COD removal rate in both cycle tests (data not shown). Figs. 2a and 2b show that a small amount of NH_4-N was removed during the non-aeration period, probably attributable to heterotrophic assimilation and adsorption by the granules (Bassin et al., 2011). In the subsequent aeration stage, NH_4-N was observed to first convert to NO_2-N and then rapidly to NO_3-N by nitrifying bacteria. Both NH_4-N and NO_2-N were not detectable (99.9% of nitrification) after influent feeding for about 2 h and 3 h under influent NH_4-N conditions of 100 mg/L and 200 mg/L, respectively (Figs. 2a and 2b). The results indicate that the granules possess excellent nitrification capacity, about 9 mg NH_4-N/g-VSS·h with the influent COD of 600 mg/L and NH_4-N of 200 mg/L.

As shown in Fig. 2a, on the other hand, phosphorus was observed to release remarkably during the non-aeration period while P uptake was detected during aeration period under 100 mg/L of influent NH_4-N concentration, suggesting the presence and activity of polyphosphate accumulating organisms (PAOs). This

phenomenon, however, didn't occur when the influent NH_4-N concentration increased to 200 mg/L (Fig. 2b), signaling the activity of PAOs might be inhibited by free ammonia (FA). Zheng et al. (2013) claimed that 8.88 mg-N/L of FA initialed the inhibition on PAOs and its toxic threshold concentration for P metabolism would be 17.76 mg-N/L. In this study, the pH of bulk liquor ranged between 7.5 and 8.0, thus FA was maintained at relatively high levels (3.6 - 11.1 mg-N/L). In addition, only about 1 mg-P/L of P removal (10% of influent P) was achieved through microbial assimilation during the two cycle tests, which was mostly associated with a long SRT (40 days) applied in this study. The above results suggest that the aerobic granules cultivated in this study possess high nitrification capability while low P removal efficiency.

3.3. P fractionation in aerobic granules by SMT protocol

Table 2 lists the analytical results of P fractions in seed sludge and aerobic granules. Seen from Table 2, it is clearly that the content of each P fraction in seed sludge is much higher than that in aerobic granules. This observation may be resulted from the different influent composition and operation strategy between the seed sludge sampled from the wastewater treatment plant and the aerobic granules cultivated in this study. Table 2 also shows that the OP content maintained at around 7.5 mg/g-MLSS in aerobic granules during the whole process, suggesting that OP is relatively stable in quantity under the designed operation conditions, which may play an important role in the P recovery from aerobic granules. Although the OP content of

seed sludge (15.6 mg/g) is much higher than that of granules (Table 2), the percentage of OP to TP for both sludges is quite similar (42.3% in the seed sludge and 39.3-43.3% in the granules sampled between day 30 and day 60, Fig. 3a). Specifically, it is worth mentioning that the OP content and percentage in this study are higher than the findings of previous studies (1.4-5.8 mg/g and 9.9-22.3%)(Xie et al., 2011b; Medeiros et al., 2005), which might be brought about by the different drying and storage methods used for sludge preparation in these works.

On the other hand, IP is the major P fraction in the seed sludge (57.5% of TP) and aerobic granules (61.4%-67.7% of TP), in which NAIP amounts to 65.1% and 61.9-70.2% of IP, respectively (Fig.3a). In addition, NAIP is about 37.4% and 38.0-47.5% of TP in the seed sludge and aerobic granules. Compared with OP and NAIP, AP content is relatively lower and much stable, about 20.9% and 18.1-20.1% of TP respectively in the seed sludge and aerobic granules, respectively.

When the changes in biomass concentration in the reactors are taken into consideration, P mass stored in the sludge could be used for the assessment of P accumulation capability of the microorganisms (PAOs). Obviously from Fig. 3b it can be discerned that before granular maturation (day 30), little accumulation was detected in all the P fractions, although the biomass concentration doubled in the reactors (Table 1), possibly due to the absence of PAOs and the operation strategy used in this study. Under the same operation conditions including the same influent COD (600 mg/L) and NH_4-N (100 mg/L) concentrations, however, P amount stored in the biomass increased remarkably on day 60 by 80%, 53% and 70% with respect to

277 TP, OP and IP, respectively, although P removal from wastewater was low (Fig.2).
278 Nevertheless, this increase trend seemed to retard to some extent when the influent
279 NH_4-N concentration was increased to 200 mg/L, especially for OP. This observation
280 partly coincides with the cycle tests (Fig. 2). Along with the operation from day 60 to
281 day 120, although P mass in inorganic forms (NAIP and AP) continuously increased,
282 the organic P mass showed much less increment (Fig. 3b), partially signaling the
283 activity of PAOs was inhibited. In addition, seen from Fig. 3b the accumulation rates
284 of P species during days 30-60 were about 2 times those of P species during days
285 90-120, also suggesting PAOs in the granules might be inhibited during the later
286 period (under 200 mg/L of influent NH_4-N conditions).
287 Interestingly, the increase of IP, NAIP and AP in the sludge was found to have
288 close relationship with the amount of metal ions accumulated in the granules,
289 especially Ca and Fe in this work (Table 3). The linear correlation coefficient (R^2) was
290 0.995 between accumulated Fe and NAIP, which was about 0.971 between
291 accumulated Ca and AP content in the sludge. According to the SMT protocol, NAIP
292 is mainly associated with Al, Fe and Mn, while AP is directly related with Ca (Ruban
293 et al., 1999; Pardo et al., 2003). Due to very less amount of Mn and Al in the sludge, it
294 can be inferred that mineral phosphorus was mainly associated with Fe and Ca in
295 NAIP and AP fractions, respectively in this study. In addition, the accumulation of Fe
296 in granules has a positive effect on the bio-available P because both NAIP and OP are
297 regarded as potentially releasable and bio-available P (Ruban et al., 1999; Xie et al.,
298 2011a). As AP is considered to be non-bioavailable P, Ca accumulation or

299 precipitation will bring about an increase in quantity of AP and then a decrease in the
300 proportion of bio-available P in the granules. Furthermore, Ca precipitation is
301 supposed to have a negative effect on the accumulation of polyphosphate and OP in
302 the sludge, leading to the decreases in bioavailability of phosphorus, PAO activity and
303 MLVSS/MLSS ratios of granules (Barat et al., 2008; Ren et al., 2008). Restated, in
304 this study the IP accumulated in biomass was mainly contributed by the increase in
305 NAIP content (Fig. 3b), implying an increased bio-availability of P in the nitrifying
306 granules during the granulation process.

307 In this study, the proportion of NAIP+OP was about 80% for both seed sludge and
308 aerobic granular sludge (Fig. 3a). Similar results were reported by Xie et al. (2011b)
309 who found that NAIP+OP was greater than 85% and 75% of TP in activated sludge
310 samples fed with domestic and industrial wastewaters, respectively. Moreover, a
311 positive correlation (R^2= 0.995) was observed between TP and NAIP+OP in aerobic
312 granules during the whole operation. Therefore, it could be concluded that high
313 potentially mobile and bio-available phosphorus were stored in the nitrifying aerobic
314 granules.
315

316 **3.4. Species of inorganic P in aerobic granules by XRD**

317 XRD, an efficient tool for distinguishing crystalline minerals from those of
318 amorphous structure, was used to identify the species of P minerals in the granule
319 samples. As illustrated in Fig. 4, a number of distinct peaks in the diffractogram
320 reflect the presence of crystalline forms. By comparison with portable document
321 format standard card (2004) using Jade 6.0, most of the stronger peaks coincide with

322 those of hydroxyapatite ($Ca_5(PO_4)_3(OH)$) pattern and iron phosphate($Fe_7(PO_4)_6$)
323 pattern.
324 Different P minerals have been reported in aerobic granules, such as
325 hydroxyapatite ($Ca_5(PO4)_3(OH)$), whitlockite ($Ca_3(PO_4)_2$, $Ca_{18}Mg_2H_2(PO_4)_{14}$) and
326 struvite ($NH_4Mg\ PO_4 \bullet 6H_2O$) in previous studies (Angela et al., 2011; Li et al., 2014;
327 Lin et al., 2012). The result from this study agrees with Angela et al (2011) who
328 reported that hydroxyapatite was a major phosphate mineral in aerobic granules. In
329 the calcium phosphate family, hydroxyapatite is considered as the most stable and
330 insoluble one. Moreover, the dense structure of granules encourages the accumulation
331 of P minerals in the core of granules and represses the solubilization of the crystals.
332 However, no whitlockite ($Ca_3(PO_4)_2$) or struvite ($NH_4Mg\ PO_4 \bullet 6H_2O$) was detected in
333 the granules. As pH and influent composition play an important role on phosphate
334 precipitation due to their influence on the saturation index (SI) of different minerals
335 (Montastruc et al., 2003; Barat et al., 2011; Juang et al., 2010), in this study SI was
336 calculated using the Visual MINTEQ ver. 3.1 database (PHREEQC software) (Table
337 4). The results show that SI of struvite was negative under the designed conditions in
338 this study, indicating magnesium concentration might be too low to initiate struvite
339 precipitation. The SI of whitlockite ($Ca_3(PO_4)_2$) was close to zero, implying
340 whitlockite was poorly or very temporarily formed. On the contrary, high level of SI
341 (between 4.78 and 7.66) was obtained for hydroxyapatite, i.e. the most stable phase
342 among the calcium phosphates signaling its oversaturation state in the tested
343 conditions. Besides the naturally chemical precipitation of hydroxyapatite, biological

especially PAOs induced hydroxyapatite precipitation and accumulation should also be considered (Angela et al., 2011). As mentioned above, the accumulation rate of AP during days 30-60 was much higher than that during days 90-120. To some extent, the increased AP content might be partially contributed by PAOs induced hydroxyapatite precipitation, due to that hydroxyapatite is the major component of AP.

In addition, high level of SI for vivianite ($Fe_3(PO_4)_2 \cdot 8H_2O$) was also obtained (Table 4). According to the portable document format standard card, the observed XRD peaks do not agree with those of vivianite ($Fe_3(PO_4)_2 \cdot 8H_2O$) pattern. However, two major peaks (20.5 and 29.7) of the granular sample could be assigned to another iron phosphate, ($Fe_7(PO_4)_6$ pattern. Under the high DO levels (7-9 mg/L) applied in the reactors in this study, part of Fe^{2+} could be inevitably and easily oxidized to Fe^{3+} and then formed the stable crystal of iron phosphate($Fe_7(PO_4)_6$). Moreover, $FePO_4$ crystal can be gradually transformed into iron phosphate ($Fe_7(PO_4)_6$) by redox reactions (Gadgil et al., 1994; Wang et al., 2013) created in the granules. Therefore, it can be confirmed that hydroxyapatite (HAP) and iron phosphate ($Fe_7(PO_4)_6$) are the major inorganic P in the nitrifying aerobic granules in this study. Still, whether other intermediates present or not remain unknown due to the limitation of XRD for micro-amount minerals.

3.5. Identification of P species in granules by ^{31}P NMR analysis

All NMR-spectra show peaks in the areas for orthophosphate (Ortho-P, 5–7 ppm), orthophosphate monoesters (Monoester-P, 3–5 ppm), orthophosphate diester

366 (Diester-P, 2 to −3 ppm), pyrophosphate (Pyro-P, −4 to −6 ppm), polyphosphate
367 (Poly-P, −18 to −21 ppm), and phosphonates (22–24 ppm) (Fig. 5). Monoester-P,
368 Diester-P and phosphonates belong to OP, while Ortho-P, Pyro-P and Poly-P are IP.
369 Although it's difficult to make an exact integration of the peak areas in NMR, the
370 quantification of these compounds with NMR is a suitable method to estimate the
371 relative proportions of P groups (Ahlgren et al., 2005; Zhang et al., 2013). Table 5
372 shows the contents of these P fractions extracted by NaOH+ Na_2EDTA method and
373 their relative proportions (%TP) identified by ^{31}P NMR. The average TP content in the
374 NaOH+ Na_2EDTA extracts was 17.3 mg-P/g SS with an average extraction rate of
375 approximately 77.6% of TP, which is similar with the result (about 73%) obtained by
376 Turner et al.(2004).
377 Orthophosphate is the dominant P species in the granule extracts, accounting for
378 74.3% of TP. Ortho-P mainly exists in phosphate form like Fe- and Ca-bound
379 inorganic P and is also the main nutrient for living organisms. It is deduced that
380 accumulation of Fe and Ca could increase the concentration of orthophosphate in the
381 granules. Although a low level of 1.9% (of TP) was detected in the granule extracts,
382 Pyro-P content in the granules is much higher than those (0.2-0.8%) of lake sediment
383 samples (Zhang et al., 2013). Besides, the presence of Pyro-P signals high microbial
384 activity involved in the biological P cycling in samples (Condron et al., 1985; Ahlgren
385 et al., 2005). On the other hand, only a very small amount of Poly-P was extracted,
386 comprising approximately 0.1% of the extractable TP from granules, which is much
387 lower than those (50% of TP) from activated sludge samples with

388 phosphate-accumulating bacteria (Uhlmann, et al., 1990). The less amount of Poly-P
389 in the granules sampled on day 120 was probably brought about by the inhibition of
390 FA on the activity of PAOs. Extracellular polymeric substances (EPS) was noticed to
391 play an important role on P species in EBPR sludge (Zhang et al., 2013a, 2013b), in
392 which Poly-P was the major P species followed by Ortho-P and Pyro-P. In this study,
393 Poly-P was much lower, about 0.1% of the extractable TP, compared to other IP
394 species like Ortho-P and Pyro-P determined. Thus much less contribution of Poly-P
395 was associated with the change in P bioavailability of the nitrifying granules, possibly
396 due to the inhibition of FA to PAOs, which needs further investigation. Furthermore,
397 EPS, consisting of polysaccharides, proteins, glycoproteins, nucleic acids,
398 phospholipids, and humic acids (Adav et al., 2008b; McSwain et al., 2005), can form
399 a matrix for microbial cells and influence the distribution of poly-P and OP species in
400 the granules.

401 On the other hand, Monoester-P is the major form of OP extracted with NaOH-
402 Na_2EDTA from the aerobic granules, accounting for about 21.8% of TP. This is in
403 agreement with the previous results from soil and sediment samples. Monoester-P can
404 be directly correlated with microbial, for instance, the glycerol-6-phoshate
405 (nucleotides) found in cell membrane belongs to Monoester-P (Ahlgren et al., 2011).
406 In addition, George et al. (2006) reported that the rhizosphere of plant could utilize
407 Monoester-P from oxisols after phosphatase hydrolysis. Moreover, algae can
408 assimilate more than 40% of P from Monoester-P in a temperate mesotrophic lake
409 (Hernandez et al., 1997). Although only 1.8% of extracted TP in granules, Diester-P

plays a crucial role in the aerobic granules due to its close relation to deoxyribonucleic acid (DNA-P), lipid (lipids-P) and teichoic acid (Teichoic-P). Thus the quantity of Diester-P can be used to indicate the activity and concentration of microorganisms in aerobic granules. As Whitton et al. (1991) pointed out that Diester-P could be easily absorbed and utilized by plants and blue green algae under certain conditions, the OP fractions including Monoester-P and Diester-P are believed to play an important role in the potential mobility and bio-availability of P resource from aerobic granular sludge.

4. Conclusion

This study presents the preliminary results of P species and its bio-availability in nitrifying aerobic granular sludge. The following major conclusions could be arrived at:

(1) IP is the primary P fraction in the granules, in which NAIP amounts to 62-70%. A positive strong correlation (R^2=0.971-0.995) has been found between the content of IP (NAIP and AP) and that of metal ions (especially Fe and Ca) in the granules. OP content was very stable in quantity during the operation. About 80% of TP in aerobic granular sludge possessed high potential mobility and bio-availability.

(2) XRD analysis and SI calculation reveal that hydroxyapatite ($Ca_5(PO_4)_3(OH)$) and iron phosphate($Fe_7(PO_4)_6$) patterns are the main IP species in the nitrifying aerobic granules.

(3) Three organic P compounds (Monoester-P, Diester-P, phosphonates) and three

inorganic P compounds (Ortho-P, Pyro-P and Poly-P) have been identified by using ^{31}P NMR, respectively. Monoester-P was the dominant P in OP, and less amount of Poly-P was detected in the granules, probably attributable to the inhibition of FA on the activity of PAOs.

In this study P removal rate was low due to the inhibition of relatively high FA levels, which could be alleviated with enhanced P removal by adjusting operation strategy (data not shown). The results from current work imply that aerobic granules could be further potentially developed as P resource materials with high amount of bioavailable P.

References

Adav, S.S., Lee, D.-J., Show, K.-Y., Tay, J.-H., 2008a. Aerobic granular sludge: recent advances. Biotechnology Advances 26 (5), 411-423.

Adav, S.S., Lee, D.-J., Tay, J.-H., 2008b. Extracellular polymeric substances and structural stability of aerobic granule. Water Research 42 (6-7), 1644-1650.

Ahlgren, J., Reitzel, K., Brabandere, H.D., Gogoll, A., Rydin, E., 2011. Release of organic P forms from lake sediments. Water Research 45 (2), 565-572.

Ahlgren, J., Tranvik, L., Gogoll, A., Waldeback, M., Markides, K., Rydin, E., 2005. Sediment depth attenuation of biogenic phosphorus compounds measured by ^{31}P NMR. Environmental Science & Technology 39 (3), 867-872.

Angela, M., Beatrice, B., Mathieu, S., 2011. Biologically induced phosphorus precipitation in aerobic granular sludge process. Water Research 45 (12), 3776

-3786.

APHA, 1998. Standard Methods for the Examination of Water and Wastewater, 20th ed. American Public Health Association/American Water Work Association/Water Environment Federation, Washington D.C., USA.

Barat, R., Montoy,T., Borrás, L., Ferrer, J., Seco, A., 2008. Interactions between calcium precipitation and the polyphosphate-accumulating bacteria metabolism. Water Research 42 (13), 3415-3424.

Barat, R., Montoya, T., Seco, A., Ferrer, J., 2011. Modelling biological and chemically induced precipitation of calcium phosphate in enhanced biological phosphorus removal systems. Water Research 45 (12), 3744-3752.

Bassin, J.P., Pronk, M., Kraan, R., Kleerebezem, R., and van Loosdrecht, M.C.M., 2011. Ammonium adsorption in aerobic granular sludge, activated sludge and anammox granules. Water Research 45 (16), 5257-5265.

Cordell, D., Drangert, J.-O., White, S., 2009. The story of phosphorus: Global food security and food for thought. Global Environmental Change 19 (2), 292-305.

Condron, L.M., Goh, K.M., Newman, R.H., 1985. Nature and distribution of soil phosphorus as revealed by a sequential extraction method followed by 31P nuclear magnetic resonance analysis. Journal of Soil Science 36 (2), 199-207

Gadgil, M., Kulshreshtha, S., 1994. Study of $FeSO_4$ catalyst. Journal of Solid State Chemistry 111, 357-364.

George, T.S., Turner, B.L., Gregory, P.J., Menun, C.B.J., Richardson, A.E., 2006. Depletionoforganic phosphorus from Oxisols in relation to phosphatase activities

476 in the rhizosphere. European Journal of Soil Science 57 (1), 47-57.
477 Hernandez, I., Christmas, M., Yelloly, J.M., et al., 1997. Factors affecting surface
478 alkaline phosphatase activity in the brown alga focus spiralis at a North Sea inter
479 tidal site (Tyne sands, Scotland). Journal of Phycology 33 (4), 569-575.
480 Juang Y.-C., Adav, S. S., Lee, D.-J., Tay, J.-H., 2010. Stable aerobic granules for
481 continuous-flow reactors: Precipitating calcium and iron salts in granular
482 interiors. Bioresource Technology 101 (21), 8051-8057.
483 Li, M., Zhang, J., Wang G., Yang H., Whelan, M.J., White, S. M., 2013. Organic
484 phosphorus fractionation in wetland soil profiles by chemical extraction and
485 phosphorus-31 nuclear magnetic resonance spectroscopy. Applied Geochemistry
486 33, 213-221.
487 Li, Y., Zou J., Zhang, L., Sun J., 2014. Aerobic granular sludge for simultaneous
488 accumulation of mineral phosphorus and removal of nitrogen via nitrite in
489 wastewater. Bioresource Technology 154, 178-184.
490 Lin, Y.M., Bassin, J.P, Van Loosdrecht, M.C.M., 2012. The contribution of
491 exopolysaccharides induced struvites accumulation to ammonium adsorption in
492 aerobic granular sludge. Water Research 46 (4), 986-992.
493 McSwain, B.S., Irvine, R.L., Hausner, M., Wilderer, P.A., 2005. Composition and
494 distribution of extracellular polymeric substances in aerobic flocs and granular
495 sludge. Applied and Environmental Microbiology 71 (2), 1051-1057.
496 Medeiros, J.J.G., Cid, B.P., Gomez, E.F., 2005. Analytical phosphorus fractionation
497 in sewage sludge and sediment samples. Analytical and Bioanalytical Chemistry

381 (4), 873-878.

Montastruc, L., Azzaro-P.C., Biscans, B., Cabassud, M., Domenech, S., 2003. A thermochemical approach for calcium phosphate precipitation modeling in a pellet reactor. Chemical Engineering Journal 94 (1), 41-50.

Pardo, P., Lopez-S, F.F., Rauret, G., 2003. Relationships between phosphorus fractionation and major components in sediments using the SMT harmonised extraction procedure. Analytical and Bioanalytical Chemistry 376 (2), 248-254.

Qin, L., Tay, J.-H., Liu, Y., 2004. Selection pressure is a driving force of aerobic granulation in sequencing batch reactors. Process Biochemistry 39 (5), 579-584.

Ren,T.-T., Liu,L., Sheng, G.-P., Liu, X.-W., Yu, H.-Q., Zhang, M.-C., Zhu, J.-R., 2008. Calcium spatial distribution in aerobic granules and its effects on granule structure, strength and bioactivity. Water Research 42 (13), 3343-3352.

Ruban, V., Lopez-Sanchez, J.F., Pardo, P., Rauret, G., Muntau, H., Quevauviller, P., 1998. Selection and evaluation of sequential extraction procedures for the determination of phosphorus forms in lake sediment. Journal of Environmental Monitoring 1, 51-56.

Singh, R.P., Agrawal, M., 2008. Potential benefits and risks of land application of sewage sludge. Waste Manage 28 (2), 347-358.

Turner, B.L., Mahieu, N., Condron, L.M., 2003. Phosphorus-31 nuclear magnetic resonance spectral assignments of phosphorus compounds in soil NaOH–EDTA extracts. Soil Science Society of America Journal 67, 497-510.

Turner, B.L., 2004. Optimizing phosphorus characterization in animal manures by

520 solution phosphorus- 31 nuclear magnetic resonance spectroscopy. Journal of
521 Environmental Quality 33(2), 757-766.
522 Uhlmann, D., Roske, I., Hupfer, M., Ohms, G., 1990. A simple method to distinguish
523 between polyphosphate and other phosphate fractions of activated sludge. Water
524 Research 24(11), 1355-1360.
525 Verawaty, M., Tait, S., Pijuan, M., Yuan, Z., Bond, P. L., 2013. Breakage and growth
526 towards a stable aerobic granule size during the treatment of wastewater. Water
527 Research 47 (14), 5338-5349.
528 Wang, R., Lin, R., Ding, Y., Liu, J., Wang, J., Zhang, T., 2013. Structure and phase
529 analysis of one-pot hydrothermally synthesized $FePO_4$-SBA-15 as an extremely
530 stable catalyst for harsh oxy-bromination of methane. Applied Catalysis A:
531 General 453 (26), 235-243.
532 Whitton, B.A., Grainger, S.L.J., Hawley, G.R., et al., 1991. Cell bound and extra
533 cellular phosphatase activities of cyanobacterial isolates. Microbial Ecology 21
534 (1), 85-98.
535 Xie, C., Tang, J., Zhao, J., Wu, D., Xu, X., 2011a. Comparison of phosphorus
536 fractions and alkaline phosphatase activity in sludge, soils, and sediments.
537 Journal of Soils and Sediments 11 (8), 1432-1439.
538 Xie, C., Zhao, J., Tang, J., Xu, J., Lin, X., Xu X., 2011b. The phosphorus fractions
539 and alkaline phosphatase activities in sludge. Bioresource Technology 102 (3),
540 2455-2461.
541 Xu H., Zhang, H., Shao, L., He P., 2012. Fraction distributions of phosphorus in

sewage sludge and sludge ash. Waste Biomass Valorization 3 (3), 355-361.

Yilmaz, G., Lemaire, R., Keller, J., Yuan, Z.G., 2008. Simultaneous nitrification, denitrification, and phosphorus removal from nutrient-rich industrial wastewater using granular sludge. Biotechnology and Bioengineering 100 (3), 529-541.

Zhang, H.-L., Fang W., Wang, Y.-P., Sheng, G.-P., Zeng, R.J., Li, W.-W., Yu, H.-Q., 2013a. Phosphorus removal in an enhanced biological phosphorus removal process: roles of extracellular polymeric substances. Environmental Science & Technology 47(20), 11482-11489.

Zhang, H.-L., Fang W., Wang, Y.-P., Sheng, G.-P., Xia, C.-W., Zeng, R.J., Yu, H.-Q., 2013b. Species of phosphorus in the extracellular polymeric substances of EBPR sludge. Bioresource Technology 142, 714-718

Zhang, L., Wang, S., Jiao, L., Ni, Z., Xia, H., Liao, J., Zhu, C., 2013. Characteristics of phosphorus species identified by ^{31}P NMR in different trophic lake sediments from the Eastern Plain, China. Ecological Engineering 60, 336-343.

Zheng, X., Sun, P., Lou J., Cai, J., Song, Y., Yu, S., Lu, X., 2013. Inhibition of free ammonia to the granule-based enhanced biological phosphorus removal system and the recoverability. Bioresource Technology 148, 343-351.

559 **Tables**

560

Operation duration (day)	MLSS (g/L)	MLVSS/MLSS (%)	SVI$_{30}$ (ml/g)	Average diameter (mm)
0	3.6	80	81	0.17
30	7.8	86	28	0.38
60	11.5	82	25	0.62
90	12.8	77	22	0.76
120	13.1	73	22	0.78

561

562

Operation duration (day)	TP	OP	IP	NAIP	AP	NAIP+AP
Seed sludge	36.9±0.9	15.6±0.5	21.2±0.7	13.8±0.5	7.7±0.3	21.5±0.8
30	17.1±0.4	7.4±0.5	10.5±0.3	6.5±0.4	3.1±0.2	9.6±0.7
60	19.6±0.7	7.7±0.3	12.1±0.6	8.0±0.6	3.7±0.2	11.7±0.7
90	20.4±0.6	7.3±0.6	13.5±0.5	9.2±0.4	4.1±04.	13.3±0.5
120	22.3±0.6	7.6±0.4	15.1±0.2	10.6±0.5	4.4±0.3	15.0±0.6

The data are expressed as mean value ± standard deviation. MLSS, mixed liquor suspended solids; TP, total phosphorus; OP, organic phosphorus; IP, inorganic phosphorus; NAIP, non-apatite inorganic phosphorus; AP, apatite phosphorus.

563

564

Operation duration (day)	Na	K	Ca	Mg	Fe	Mn	Al
30	3	1	4	2	6	0	0
	.71	.46	.60	.67	.02	.21	.15
60	4	2	6	3	8	0	0
	.05	.06	.77	.74	.07	.26	.18
90	4	2	8	3	1	0	0
	.27	.33	.49	.51	0.46	.31	.25
120	5	3	1	3	1	0	0
	.50	.07	0.79	.96	2.48	.45	.25

565

566

Species	100 mg NH_4-N /L		200 mg NH_4-N /L	
	pH 7.5	pH 8.0	pH 7.5	pH 8.0
$Ca_3(PO_4)_2$ (beta)	-0.63	0.47	-1.08	-0.01
Calcite($CaCO_3$)	-0.42	0.08	-0.25	0.25
Dolomite ($CaMg(CO_3)_2$)	-0.76	0.24	-0.41	0.59
Hydroxyapatite($Ca_5(PO_4)_3(OH)$)	5.53	7.66	4.78	6.89
Struvite($MgNH_4PO_4 \cdot 6H_2O$)	-1.81	-1.26	-1.69	-1.15
Vivianite ($Fe_3(PO_4)_2 \cdot 8H_2O$)	6.26	7.35	6.24	7.33

567

568

TP	IP			OP		
(mg/g-SS)	Ortho-P (%)	Pyro-P (%)	Poly-P (%)	Monoester-P (%)	Diester-P (%)	Phosphonate (%)
17.3	74.3	1.9	0.1	21.8	1.8	0.1

SS, suspended solids; Ortho-P, orthophosphate; Monoester-P, orthophosphate monoesters; Diester-P, orthophosphate diester; Pyro-P, pyrophosphate; Poly-P, polyphosphate.

569

570

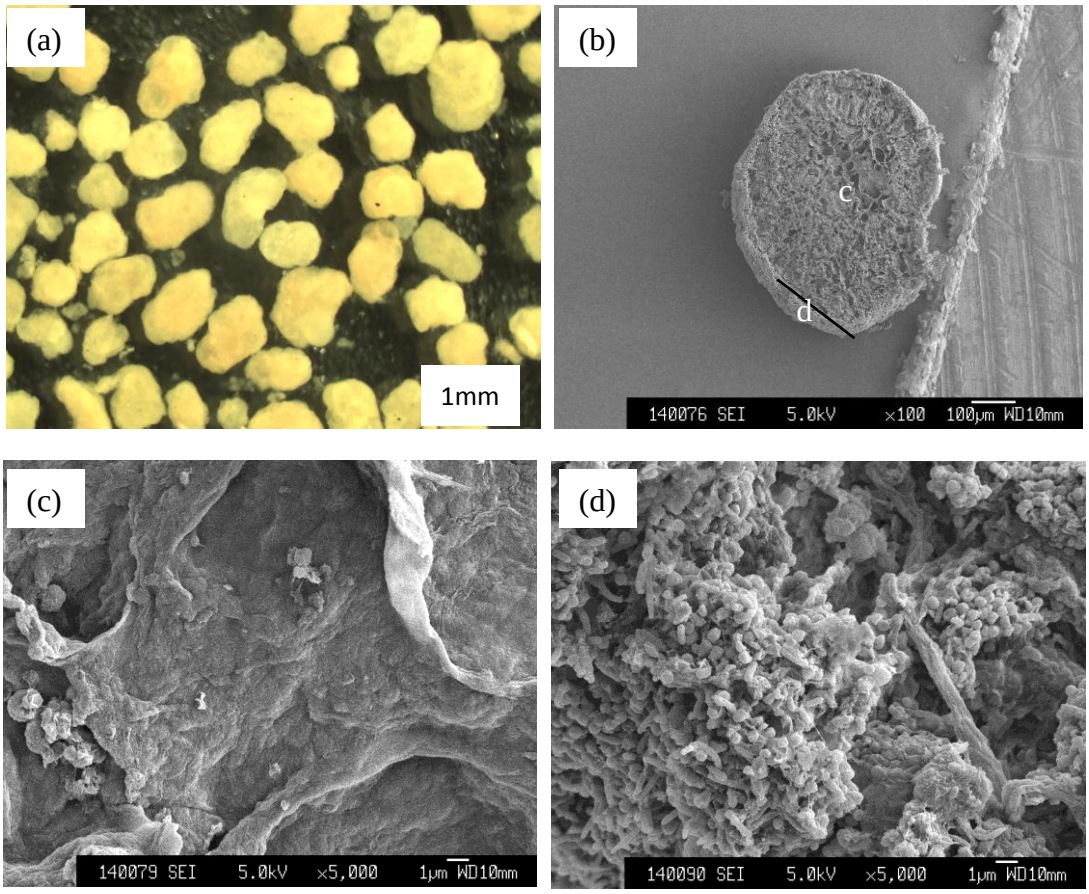

571

572

573

574 Fig. 1 – Images of the granular sludge on day 110 (Influent NH_4-N= 200 mg/L).
575 Digital image of granules (a), and SEM observation of granules from cross section (b),
576 core (c) and edge (d) on day 110, respectively.

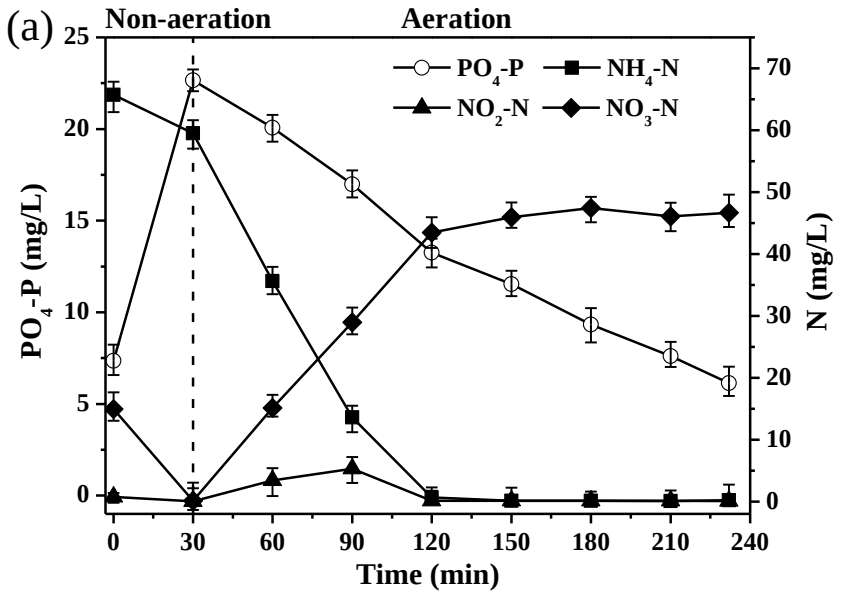

577

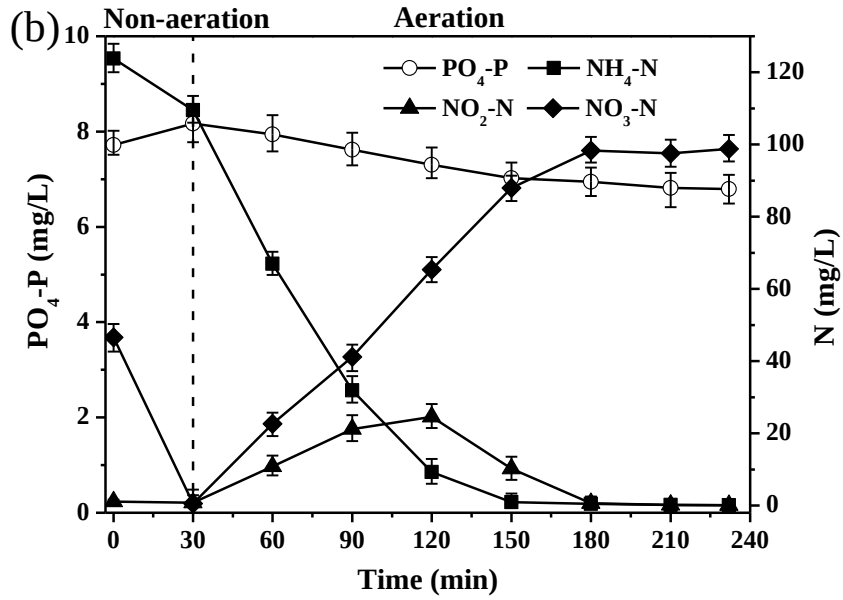

578
579
580

581 Fig. 2 – Variation of NH_4-N, NO_2-N, NO_3-N and PO_4-P in the bulk liquor during
582 cycle tests under 100 mg/L (a) and 200 mg/L (b) of influent NH_4-N concentration,
583 respectively.

584

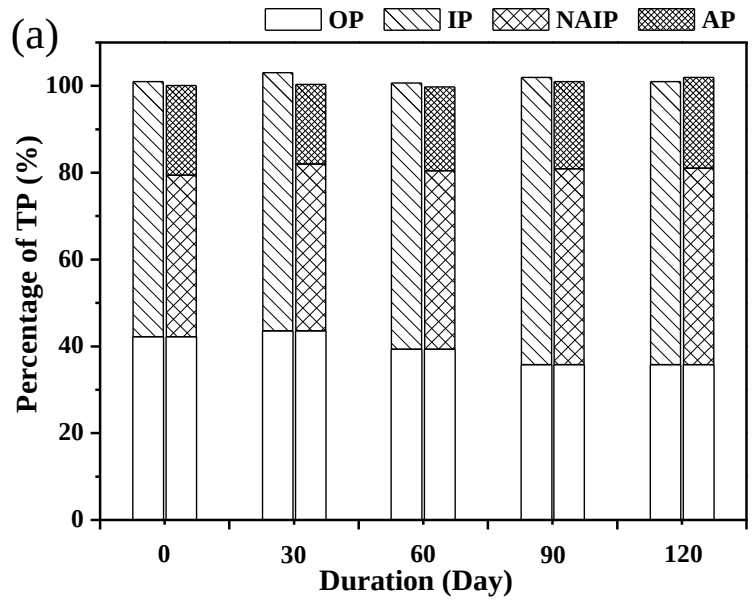

585

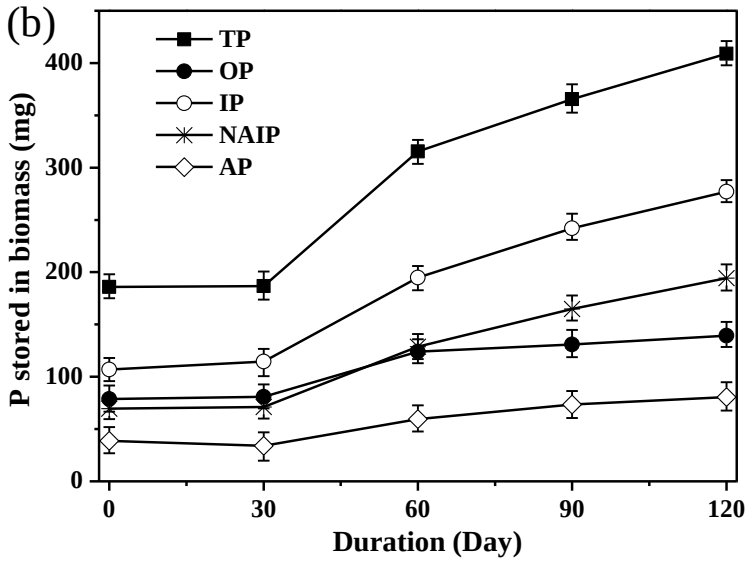

586

587

588 Fig. 3 – Average proportions of phosphorus fractions (%TP) in sludge (a) and changes
589 in P mass stored in biomass in the reactors (b) during 120 days' operation. TP, total
590 phosphorus; OP, organic phosphorus; IP, inorganic phosphorus; NAIP, non-apatite
591 inorganic phosphorus; AP, apatite phosphorus. P stored in biomass is estimated
592 according to P fraction content and biomass (MLSS) concentration in the reactors.

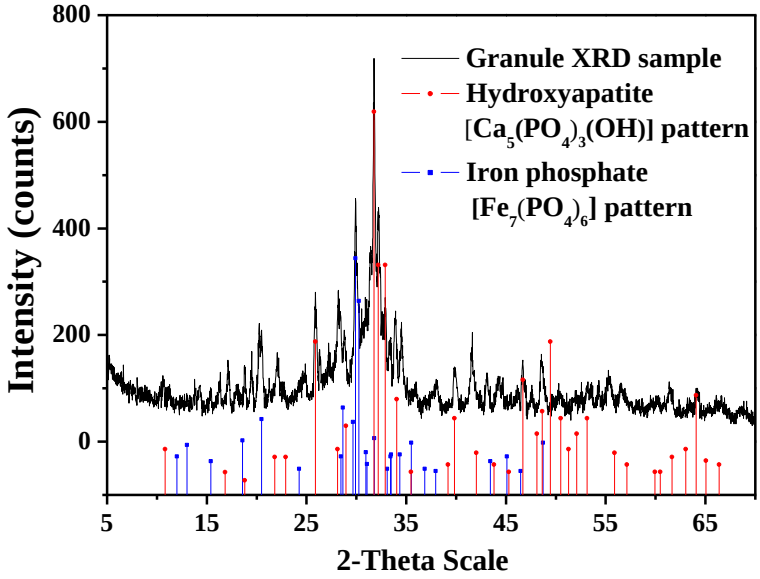

593

594

595 Fig. 4 – XRD diffractogarm of granular sludge compared to standard hydroxyapatite
596 and iron phosphate patterns

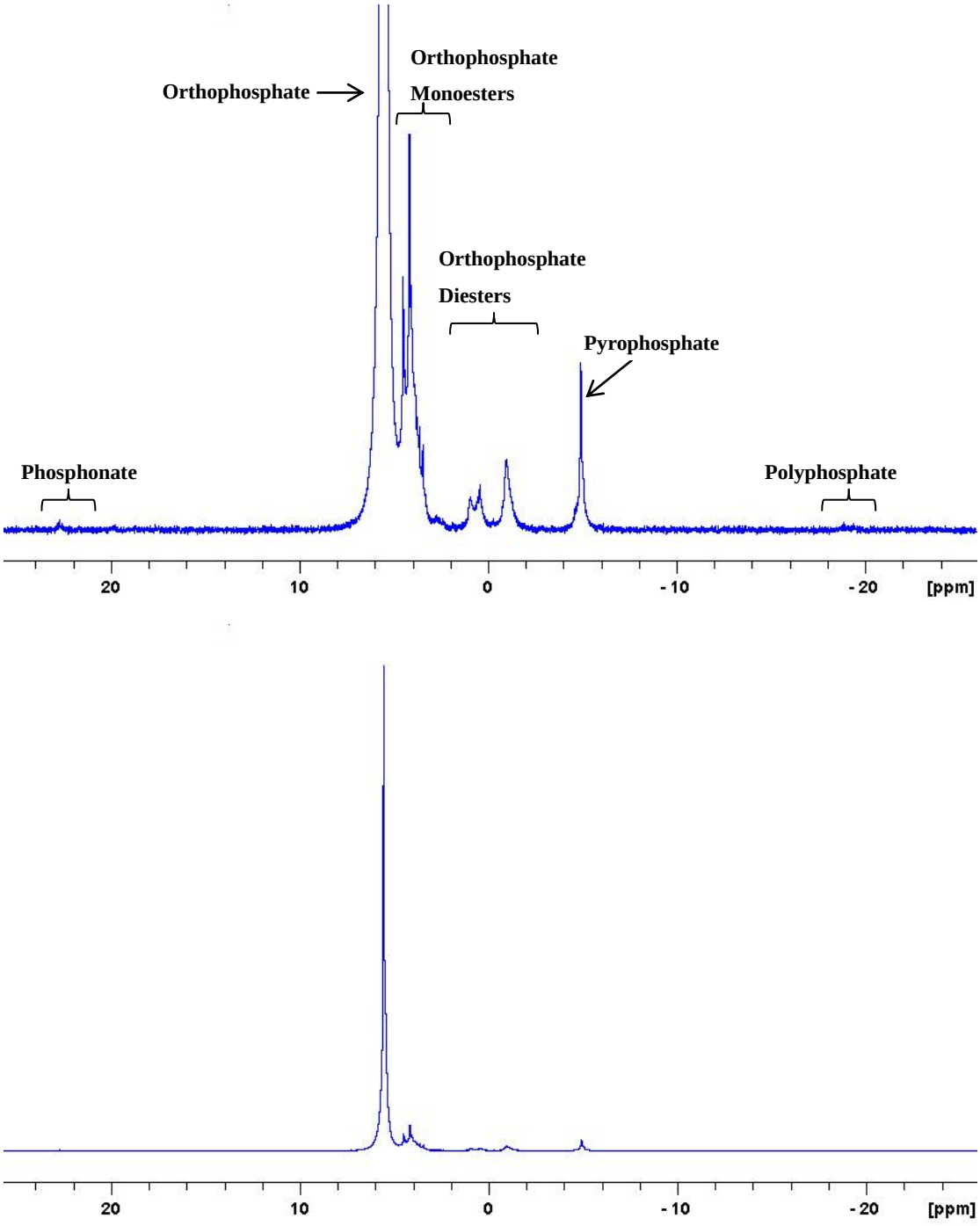

Fig. 5 – Typical ^{31}P-NMR spectra of NaOH+Na_2EDTA extracts from the aerobic granules sampled on day 120